Host Immune and Apoptotic Responses to Avian Influenza Virus H9N2 in Human Tracheobronchial Epithelial Cells

Zheng Xing[1,3], Richart Harper[2], Jerome Anunciacion[1], Zengqi Yang[4], Wei Gao[3], Bingqian Qu[3], Yi Guan[5], and Carol J. Cardona[1]

[1]Department of Population Health and Reproduction, School of Veterinary Medicine, and [2]Division of Pulmonary Medicine, School of Medicine, University of California at Davis, Davis, California; [3]Medical School and State Key Laboratory of Pharmaceutical Biotechnology, Nanjing University, Nanjing, Jiangsu, China; [4]College of Veterinary Medicine, Northwest Agriculture & Forest University, Yangling, China; and [5]State Key Laboratory of Emerging Infectious Diseases and Department of Microbiology, Li Ka Shing Faculty of Medicine, University of Hong Kong, Hong Kong, China

The avian influenza virus H9N2 subtype has circulated in wild birds, is prevalent in domestic poultry, and has successfully crossed the species boundary to infect humans. Phylogenetic analyses showed that viruses of this subtype appear to have contributed to the generation of highly pathogenic H5N1 viruses. Little is known about the host responses to H9N2 viruses in human airway respiratory epithelium, the primary portal for viral infection. Using an apically differentiated primary human tracheobronchial epithelial (TBE) culture, we examined host immune responses to infection by an avian H9N2 virus, in comparison with a human H9N2 isolate. We found that IFN-β was the prominent antiviral component, whereas interferon gamma-induced protein 10 kDa (IP-10), chemokine (C-C motif) ligand (CCL)-5 and TNF-α may be critical in proinflammatory responses to H9N2 viruses. In contrast, proinflammatory IL-1β, IL-8, and even IL-6 may only play a minor role in pathogenicity. Apparently Toll-like receptor (TLR)-3, TLR-7, and melanoma differentiation–associated gene 5 (MDA-5) contributed to the innate immunity against the H9N2 viruses, and MDA-5 was important in the induction of IFN-β. We showed that the avian H9N2 virus induced apoptosis through the mitochondria/cytochrome c–mediated intrinsic pathway, in addition to the caspase 8–mediated extrinsic pathway, as evidenced by the cytosolic presence of active caspase 9 and cytochrome c, independent of truncated BH3 interacting domain death agonist (Bid) activation. Further, we demonstrated that FLICE-like inhibitory protein (FLIP), an apoptotic dual regulator, and the p53-dependent Bcl-2 family members, Bax and Bcl-x_s, appeared to be involved in the regulation of extrinsic and intrinsic apoptotic pathways, respectively. The findings in this study will further our understanding of host defense mechanisms and the pathogenesis of H9N2 influenza viruses in human respiratory epithelium.

Keywords: avian influenza virus; H9N2; host responses; apoptosis; cytokines; chemokines; bronchial epithelial cells

CLINICAL RELEVANCE

This study characterized the host immune responses in apically differentiated primary human tracheobronchial cell culture infected with avian influenza virus H9N2. This report is the first, to the best of our knowledge, to demonstrate that both intrinsic and extrinsic apoptotic pathways are involved in apoptosis in human bronchial epithelium caused by infection with avian influenza viruses.

Avian influenza viruses (AIVs) circulate among wild birds, and have contributed critical genetic material necessary for the generation of pandemic influenza viruses. Although humans can be infected by many subtypes of AIVs, H5N1, H9N2, and H7N7 are the three that have most frequently been transmitted directly from birds to humans. The H9N2 subtype viruses were reported to be widespread in live-poultry markets in Asian countries since the late 1990s. In 1999 and 2003, H9N2 viruses were isolated from the nasopharyngeal aspirates of three children with mild symptoms in Hong Kong (1, 2). These viruses were of entirely avian origin, and were phylogenetically close to the viruses circulating in the poultry markets of Hong Kong since the late 1990s. More importantly, the six genes encoding the internal proteins of these isolates were related to the highly pathogenic H5N1 virus from birds and infected patients (3, 4). Subsequently, specific antibodies to H9N2 AIV were detected in poultry workers and patients (1, 5). These findings pointed to a possibility that AIVs such as H9N2 could infect humans directly, without acquiring human or mammalian influenza genes in an intermediate host, and emerge as or contribute to the reemergence of highly pathogenic viruses (3, 4, 6–8).

Human respiratory tract epithelia are the entry portals of influenza virus infection, and play a key role in the initial host response. Extensive studies were performed in human bronchial and lung epithelial cells to study viral replication, early host responses, and pathogenesis with human influenza H1N1, H2N2, and H3N2, as well as avian H5N1 viruses (9–21). Although both immortalized cell lines and primary cultures were used, cell cultures were mainly submerged and nondifferentiated. This is distinct from the physiologic presentation of airway cells *in vivo*. Recently, polarized human respiratory cultures, which can be differentiated in an apical cultural condition to produce ciliated and nonciliated cells, were used to study the mechanism of cell tropism and receptor binding of influenza virus subtypes such as H1N1, H3N2, H5N1, H7N1, and H9N2 (13, 16, 22). However, little is known about human respiratory epithelial cell responses to low-pathogenic avian influenza viruses such as H9N2 that directly infect humans.

One of the host cell responses to influenza infection involves the initiation of apoptosis. Apoptosis can be triggered by both extrinsic and intrinsic pathways. Influenza virus was originally found to induce apoptosis in Madin-Darby Canine Kidney (MDCK) and Hela cells (5, 23, 24) through the caspase 8–mediated extrinsic pathway (24, 25). Human respiratory cells of nasal and bronchiolar origin underwent apoptosis induced by H3N2 infection (9). Mechanistically, although the caspase 8–mediated extrinsic pathway is well-established in influenza infection, the mitochondria/cytochrome c–mediated intrinsic pathway has not been fully substantiated in infected human

(*Received in original form April 7, 2009 and in final form December 9, 2009*)

Correspondence and requests for reprints should be addressed to Zheng Xing, Ph.D., Department of Veterinary and Biomedical Science, College of Veterinary Medicine, University of Minnesota, 1971 Commonwealth Avenue, Saint Paul, MN 55108. E-mail: zxing@umn.edu

Am J Respir Cell Mol Biol Vol 44. pp 24–33, 2011
Originally Published in Press as DOI:10.1165/rcmb.2009-0120OC on January 29, 2011
Internet address: www.atsjournals.org

respiratory epithelial cells. As previously shown, neither caspase 9 nor the intrinsic pathway was involved in human respiratory cell death (9). The nonstructural-1 (NS1) protein encoded by AIV H5N1 induced apoptosis in human lung epithelial cells via the caspase 8–dependent pathway, but did not activate caspase 9 (26).

In this study, we attempt to understand how human bronchial epithelial cells (HBEs) respond to AIV H9N2 virus. Using apically differentiated primary human tracheobronchial epithelial cultures (TBEs), we examined host antiviral and proinflammatory cytokine/chemokine responses, which may play important roles in containing the H9N2 virus and contributing to pathogenicity. To further our understanding of influenza-induced apoptosis, we examined caspase activation and regulation in H9N2-infected HBEs, and found that the mitochondria/cytochrome c–mediated intrinsic pathway is also involved in cell death. Our evidence indicates that this activation of the intrinsic pathway may not be activated by truncated BH3 interacting domain death agonist (tBid), but is regulated by the p53 signaling pathway and the p53-dependent Bcl2 family members Bax and Bcl-x_s.

MATERIALS AND METHODS

Virus and Reagents

An avian H9N2 virus, A/pheasant/CA/2373/1998 (27), and a human H9N2 virus, A/Hong Kong/2108/2003 (2), were used in the study. The viruses hereafter referred to as avian (H9N2 PH) and human (H9N2 HK) H9N2 viruses were passaged in 10-day-old specific pathogen–free embryos, and the infectious viral particles in allantoic fluid were titrated in MDCK cells with a standard plaque assay. FITC-conjugated anti-influenza A nucleoprotein (NP) antibody was a product of ViroStat (Portland, ME). Anti-nonstructural protein 1 (NS1) goat antibody (vC-20), anti FLICE-like inhibitory protein (FLIP) rabbit antibody, anti-melanoma differentiation-associated gene 5 (MDA-5) goat antibody (sc-48031), and anti-actin monoclonal antibody (SPM161) were obtained from Santa Cruz Biotechnology (Santa Cruz, CA). Anti-β-tubulin IV monoclonal antibody (clone ONS.1A6) was purchased from Sigma-Aldrich (St. Louis, MO). Anti-cleaved caspase-3, anti-cleaved caspase-6, anti-cleaved caspase-7, anti-cleaved caspase-9, anti–caspase-8, and anti-cleaved Poly (ADP-ribose) polymerase (PARP) rabbit antibodies were all from CalBiochem (La Jolla, CA). Anti-Bax rabbit (Ab-1), anti-Bcl-x_s rabbit (Ab-1), and anti-Bak monoclonal (Ab-1) antibodies were purchased from EMD Biosciences (Gibbstown, NJ). Rabbit monoclonal anti-phospho-p53 (S392) antibody was obtained from Epitomics (Burlingame, CA). Goat anti-Bid antibody was a product of R&D Systems (Minneapolis, MN).

Cell Culture from Human Tissues and Virus Infection

HBE1 cells from a papilloma virus–immortalized bronchial epithelial cell line were kindly provided by Dr. J. Yankaskas of the University of North Carolina (28). Human primary TBE cells were obtained from the University of California at Davis Medical Center (Sacramento, CA). The University of California at Davis Human Subjects Review Committee approved all procedures involving human tissue procurement. Protease-dissociated TBE cells were plated on Transwell (Corning Costar, Corning, NY) chambers (12 or 24 mm) at $1–2 \times 10^4$ cells/cm^2, in Ham's F12/Dulbecco's modified Eagle's medium (DMEM) (1:1) supplemented with insulin (5 μg/ml), transferrin (5 μg/ml), epidermal growth factor (10 ng/ml), 8 dexamethasone (0.1 μM), cholera toxin (10 ng/ml), bovine hypothalamus extract (15 μg/ml), and BSA (0.5 mg/ml). After 1 week, TBE cultures were transferred to air–liquid interface (ALI) culture conditions for an additional week before infection. HBE1 cells were grown in six-well plates (Corning Costar) and maintained in the Ham's F12/DMEM medium.

To infect TBE cells, the viruses in a 100-μl volume, suspended in the culture medium, were added to the Transwell cultures at a multiplicity of infectivity (m.o.i.) of approximately 1. The apical surface of TBE cultures was washed 10 times to remove mucins before infection. Cells were incubated with the virus at 37°C for 60 minutes. After incubation, the viruses were removed, and the cells were washed twice with the culture medium. Fifty microliters of the culture medium were finally added to the apical phase of the culture. HBE1 cells were infected with the viruses at an m.o.i. of 1 in 1 ml culture medium, after a period of absorption at 37°C for 60 minutes. The viruses were discarded after the absorption, and cells were washed twice before 2 ml of the culture medium were added to each well in a six-well Costar plate. The infections for both TBE and HBE1 cells were performed in an incubator at 37°C supplied with 5% CO_2.

Immunofluorescence, Terminal Deoxynucleotidyl Transferase dUTP Nick End Labeling Staining, and IFN-β ELISA

TBE and HBE1 cells were fixed with 4% paraformaldehyde for 30 minutes and permeablized with 0.1% Triton X-100 on ice for 5 minutes, followed by washes with PBS. Air-dried cells were incubated with anti-human β-tubulin IV monoclonal antibody at a 1:100 dilution, at 37°C, for 30 minutes. After three washes with PBS, cells were incubated with rhodamine-conjugated goat anti-mouse IgG (H+L; Jackson ImmunoResearch (West Grove, PA)) at a 1:25 dilution, at 37°C, for 30 minutes, followed by three PBS washes. Cells were further incubated with FITC-conjugated anti-influenza A virus NP at a 1:50 dilution, at 37°C, for 30 minutes. After three washes with PBS, cells were air-dried, mounted with antifade reagent (8% propyl gallate in 70% glycerol), and observed with a Nikon Eclipse E600 fluorescence microscope.

For Terminal Deoxynucleotidyl Transferase dUTP Nick End Labeling (TUNEL) staining, TBE and HBE1 cells were fixed with 2% paraformaldehyde and permeablized with 0.1% Triton X-100, as described previously (29). Air-dried cells were incubated with a mixture of FITC-labeled dUTP and terminal deoxynucleotidyl transferase (TdT) polymerase, prepared as instructed by the manufacturer (Roche Diagnoistics, Indianapolis, IN) at 37°C for 60 minutes, followed by three washes of PBS. After being air-dried, cells were mounted with the anti-fade reagent and observed via fluorescence microscopy.

We used a capture ELISA reagent kit (PBL Biochemical Laboratories, Piscataway, New Jersey) to measure levels of secreted IFN-β protein in the culture supernatant of uninfected and H9N2-infected HBE1 cells, according to the manufacturer's protocol. Data were normalized according to the total protein quantities of the samples.

Real-Time RT-PCR

The mRNA levels for human IFN-α, IFN-β, IFN-γ, IL-1β, IL-6, IL-8, TNF-α, Fas ligand (FasL), TNF-related apoptosis-inducing ligand (TRAIL), Interferon gamma-induced protein 10 kDa (IP-10), chemokine (C-C motif) ligand (CCL)-5, Toll-like receptor (TLR)-3, TLR-7, TLR-8, MDA-5, and glyceraldehyde-3-phospate dehydrogenase (GAPDH) genes in uninfected and infected TBE and HBE1 cultures were analyzed by two-step, real-time RT-PCR. One microgram of total RNA, prepared from cells with the RNeasy kit (Qiagen, Valencia, CA), was used for the reverse transcription (RT) reaction with the QuantiTect Reverse Transcription Kit (Qiagen), following the manufacturer's instructions. The RT reaction was performed after the RNA had been treated with DNase I to eliminate genomic DNA contamination at 42°C for 2 minutes. Real-time PCR was conducted with 1 μl cDNA in a total volume of 25 μl with the iQ SYBR Green Supermix (Bio-Rad, Hercules, CA), following the provided instructions. The reaction was performed in an ABI 7500 Real Time PCR System (Applied Biosystems, Carlsbad, CA) for 40 cycles. Relative expression values were normalized using internal GAPDH controls. Fold changes of relative gene expression levels were calculated according to the formula: $2^{(\Delta C \text{ t of gene} - \Delta C \text{ t of GAPDH})}$. Melting curves were analyzed to determine the specificity of each reaction to the target. Reactions were conducted in duplicate and repeated at least three times for each sample, and the mean values and standard deviations were calculated. The sequences for the primers used in real-time RT-PCR were chosen using the web-based software Primer3 (version 0.4.0; http://frodo.wi.mit.edu/primer3/input.htm).

Flow Cytometric Analysis of Apoptosis

HBE1 and TBE cells infected with H9N2 virus were trypsinized and washed three times with PBS (0.5% BSA). We used 1×10^6 cells for staining with fluorescein-conjugated annexin V and propidium iodide (PI) (BD Pharmingen, San Diego, CA) in a volume of 100 μl on ice for

30 minutes. Cells were washed three times with PBS (0.5% BSA), followed by flow cytometric analysis on a FACScan cell sorter (Becton-Dickinson, San Jose, CA).

Subcellular Protein Extraction and Western Blot Analysis

Subcelluar protein extraction was performed using a ProteoExtract Subcellular Proteome Extraction Kit (Calbiochem, La Jolla, CA), following the manufacturer's instructions. The extraction was performed on ice and provided cytosol membrane/organelle and nucleus fractions, which were quantified with a BCA Protein Assay Kit (Pierce, Rockford, IL). Cell lysates of various fractions were used for SDS-PAGE with resolving gel concentrations ranging from 10–15%, depending on the protein of interest. Proteins were transferred to Immuno-Blot PVDF membranes (Bio-Rad Laboratories, Hercules, CA) with a semidry Transfer Cell (Bio-Rad Laboratories), and Western blot analyses were performed in TBS-Tween 20 containing 5% nonfat milk powder. Either horseradish peroxidase-conjugated or alkaline phosphatase-conjugated secondary antibody was used. Chemoilluminate detection reagents (Amersham Biosciences, Pittsburgh, PA) or 5-bromo-4-chloro-3-indolyl phosphate/nitro blue tetrazolium (Gibco BRL, Gaithersburg, MD) were used for signal development.

Infection in HBE1 Cells in which MDA-5 Was Knocked Down by Small Interfering RNA

The endogenous MDA-5 gene was knocked down by synthetic, double-stranded, small interfering RNA (siRNA; Santa Cruz Biotechnology). HBE1 cells (2×10^5), plated in six-well culture plates in 2 ml of antibiotic-free F12 medium, were transfected with 100 nM of siRNA duplex, using transfection agent (sc-29528; Santa Cruz Biotechnology), following the manufacturer's protocol. A pool of three MDA-5 siRNAs (sc-61010; Santa Cruz Biotechnology) was included for transfection. HBE1 cells were also transfected with 100 nM of scrambled siRNA (sc-37007; Santa Cruz Biotechnology). Transfected cells were incubated at 37°C for 24 hours before cells were infected with the H9N2 virus at an m.o.i. of 1. Cultural supernatants were harvested at 6, 12, and 24 hours for IFN-β measurement by an ELISA, and for virus titration by a standard plaque assay, whereas cell lysates were prepared for 10% SDS-PAGE and Western blot analyses.

RESULTS

Susceptibility and Cytopathogenicity of Human Tracheobronchial Epithelial Cells to Avian and Human H9N2 Viruses

To examine how human airway epithelial cells respond to AIV H9N2, we infected both HBE1 and TBE cultures with the virus, as well as a human H9N2 isolate for comparison. The HBE1 cells were infected at an m.o.i. of 1, and morphologic changes were evident 10 hours after infection. Sporadic cells became positive by FITC–anti-influenza NP antibody staining at 6 hours after infection, and nearly 75% of cells became positive at 12 hours after infection (Figure 1A). HBE1 cells infected with human H9N2 (H9N2 HK) showed a similar pattern of infection. The cytopathic effects (CPEs) in HBE1 cultures infected with both avian and human H9N2 viruses increased precipitously with time as the integrity of cell membranes was obviously damaged and cells detached. The culture monolayer was severely devastated by 24–32 hours after infection (Figure 1A, or data not shown).

We cultured TBE cultures to differentiate apically as described (see Materials and Methods), and cells were maintained in these cell culture conditions for 1–2 weeks before infection. We infected TBE cells with the H9N2 viruses at $\sim$ 1 m.o.i. Similar to the HBE1 monolayer, CPEs were observed in the TBE culture within 12 hours after infection. However, CPEs progressed more slowly in TBE than in HBE1. Although obvious CPEs occurred in foci distributed diffusely throughout each culture, the monolayers remained essentially intact throughout the course of infection, up to 96 hours. The CPEs seemed to be inversely proportional to the stage of differentiation, because CPE progressed much more aggressively in less differentiated cells (Figure 1B and data not shown). Clearly, primary TBE cultures demonstrated significantly lower susceptibility to the H9N2 virus than did HBE1 cells.

To determine differences in infectivity, viral replication in HBE1 and TBE cultures was examined. Infectious viruses released into the culture media were titrated on MDCKcells. For both avian and human H9N2 viruses, higher virus titers were evident in infected HBE1 than in primary TBE cultures (Figure 1C), and the differences in virus titers between HBE1 and TBE cultures were significant at 24 and 36 hours after infection ($P < 0.05$, $n = 3$, t test). Western blot analysis showed that the NS1 protein was detected mainly in nuclear fractions of infected HBE1 and TBE cultures (Figure 1D).

Ciliated HBE1 Cells Were More Resistant to H9N2 Infection

Unlike TBE cultures, HBE1 cells were cultured as a monolayer submerged conventionally in culture medium, which does not promote airway epithelial differentiation. We found that nearly 99% of cells had no or minimal anti-β-tubulin IV antibody staining for cilia (13), which confirmed their minimally differentiated condition. Moreover, these negative-staining cells were all infected by avian H9N2 virus, as indicated by the FITC-conjugated anti-influenza NP staining (Figure 2). We observed a few cells with strong expression of β-tubulin IV (Figure 2, *white arrows*), suggesting a more differentiated phenotype. Interestingly, these individual ciliated cells were uniformly uninfected by the virus (Figure 2). These results confirm that HBE1 cells do not differentiate under the culture conditions used, but are highly susceptible to influenza A virus infection.

Antiviral Responses in TBE Cultures Infected with H9N2 Virus

Previous studies characterized cytokine and chemokine responses to influenza A infections in human respiratory epithelial cultures. However, most studies were performed with continuous immortalized cell lines without apical differentiation. To determine cytokine responses under conditions that mimic the physiologic conditions of airway respiratory epithelia, we examined gene-expression levels in apically differentiated airway epithelial cultures. We prepared total RNA from TBE cultures infected with avian and human H9N2 viruses at various time points after infection, and examined expression levels using real-time RT-PCR. As shown in Figure 3A, IFN-α was not significantly increased in H9N2-infected TBE cells, and neither was IFN-γ (data not shown). In contrast, a vigorous IFN-β response occurred. IFN-β levels increased greater than 600-fold within 6 hours after infection. Accordingly, the myxovirus resistance 1 (Mx1) gene was upregulated over 50-fold (Figure 3B), and the 2′5′-2′-5′-oligoadenylate synthetase gene was upregulated up to 40-fold (data not shown), at 24 hours after infection.

Proinflammatory Responses in TBE Cultures Infected with H9N2 Virus

We examined the expression levels of genes involved in proinflammator responses, to understand the pathogenesis of the H9N2 infection in human airway bronchial epithelia. With real-time quantitative RT-PCR, we found that both IL-1β and IL-8 were expressed at high baseline levels (based on threshold of cycle [C_T] values) in TBE cells, but neither was significantly upregulated after infection with both avian and human H9N2 viruses (Figure 4A, or data not shown). In fact, at the earliest stages of infection (within 24 hours), the

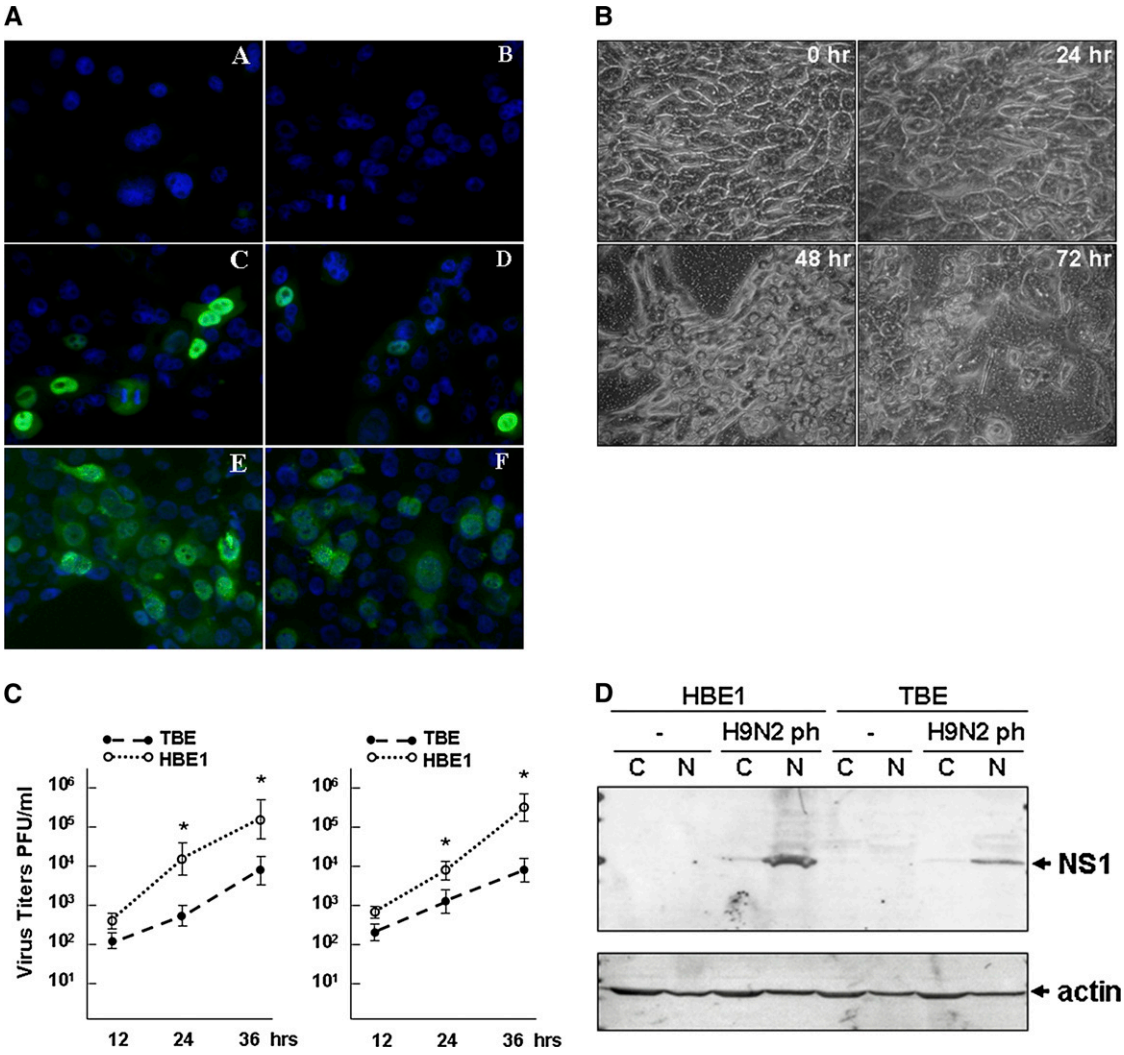

Figure 1. Susceptibility of human bronchial epithelial cells (HBEs) to avian and human H9N2 viruses. (*A*) Avian and human H9N2 infection in HBE1. Avian virus, H9N2 PH (*left*); human virus, H9N2 HK (*right*). Cells were infected with the viruses for 6 and 12 hours, respectively, and stained with an FITC–anti-influenza A nucleoprotein (NP) antibody. Subsequently fluorescence images were taken (magnification, ×200): *A* and *B*, uninfected cells; *C* and *D*, 6 hours after infection; *E* and *F*, 12 hours after infection. (*B*) Avian H9N2 infection in apically differentiated tracheobronchial epithelial cultures (TBEs). Images were taken at 0, 24, 48, and 72 hours after infection (magnification, ×400). (*C*) Replication of avian (*left*) and human (*right*) H9N2 viruses in HBE1 and TBE cultures. Infectious viruses from infected HBE1 and TBE cultures were harvested at 12, 24, and 36 hours after infection, and titrated with a standard plaque assay (*$P < 0.05$, *t* test; mean ± SEM). (*D*) Expression of nonstructural-1 (NS1) protein in HBE1 and TBE cell cultures. Cytosolic (*C*) and nuclear (*N*) fractions of cell lysates from uninfected and infected HBE1 and TBE cells, respectively, were prepared and fractionated in 15% SDS-PAGE. Cell lysates were prepared 12 hours (HBE1) and 36 hours (TBE) after infection, respectively. Western blot analyses were performed with an anti-influenza A NS1 antibody. PFU, plaque forming units.

concentrations of IL-1β and IL-8 were even downregulated to various degrees for avian H9N2 infection (Figure 4A), indicating that IL-1β and IL-8 in TBE cells were not the main proinflammatory drivers. A modest induction of IL-6 transcription, however, was observed in both avian and human H9N2-infected TBE cells.

On the other hand, chemokines IP-10 and CCL-5 vigorously increased after H9N2 infection. As shown in Figure 4B, concentrations of CCL-5 in H9N2-infected TBE cultures were upregulated up to 175-fold and 300-fold, whereas IP-10 was increased up to over 4,000-fold and 7,000-fold at 24 and 36 hours after infection, respectively. Taken together, chemokines IP-10 and CCL-5 are likely the key contributors to proinflammatory responses in human airway epithelia after H9N2 infection, whereas cytokines such as IL-6, IL-1β, or IL-8 may play minor roles.

Innate Immune Responses in H9N2 Virus–Infected TBE Cultures

To determine which innate immune mechanisms were used in H9N2-infected airway epithelial cultures, we examined the expression levels of a few membrane-bound pathogen sensor receptors. We focused on TLR-3, TLR-7, and TLR-8, which are involved in responses to RNA viruses, as well as MDA-5, a member of the cytosolic pathogen sensor receptor retinoid-inducible gene 1 family. Our data indicate that, whereas TLR-8 was almost unchanged after infection, TLR-3 and TLR-7 responded moderately, especially at time points beyond 24 hours after infection (Figures 5A and 5B). However, at the initial stages of 6 and 12 hours after infection, the concentrations of TLR-3 and TLR-7 were virtually unchanged. The concentration of TLR-7 increased up to 2.3-fold at 12 hours

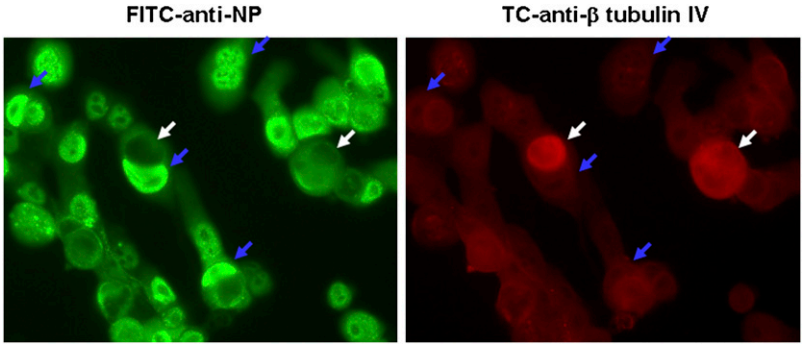

Figure 2. Differential susceptibility of HBE1 cells to avian H9N2 infection. HBE1 cells were fixed at 12 hours after infection and stained with both FITC–anti-influenza NP (*left*) and Tricolor (TC)–anti-β tubulin IV (*right*) antibodies and subjected to fluorescence microscopy (magnification, ×400). *White arrows,* β-tubulin IV–positive but viral nucleoprotein–negative; *blue arrows,* β-tubulin IV–negative but viral nucleoprotein–positive.

after infection, and to 14-fold and 48-fold at 24 and 48 hours after infection, respectively. Together, these data indicate that the RNA virus–related TLR-3 and TLR-7 receptors are responsive in H9N2-infected human airway epithelia.

On the other hand, MDA-5 was up-regulated at 6 hours after infection, and the expression levels increased up to 38-fold and 71-fold at 24 and 36 hours after infection, respectively (Figure 5B). This finding appears to indicate that cytosolic pathogen sensor receptors of the RIG-1 family may be responsive during initial stages of infection, and may be involved in combating H9N2 infection in human bronchial epithelia.

To examine the role of MDA-5 further in innate immunity against avian H9N2 infection in human bronchial epithelium, we transfected HBE1 cells with MDA-5–specific siRNA. A significant reduction of MDA-5 was evident in HBE1 cells at 24 hours after infection (Figure 6A). After avian H9N2 infection at an m.o.i of 1, IFN-β induction was detected in both siRNA and control RNA–transfected cells infected with the virus. However, a partial reduction of IFN-β induction was observed in the cultures in which MDA-5 was knocked down, which led to increased virus replication (Figures 6B and 6C).

Apoptotic Responses in H9N2-Infected HBE1 Cells

Extensive CPEs occurred in both HBE1 and TBE cultures infected with the H9N2 viruses. Most dying cells developed cytoplasmic bubbles, which is atypical for an apoptotic process (Figure 1B). Apoptosis was likely triggered in infected cells at an early stage of infection, which was subsequently followed by a necrotic process. To verify that apoptosis did occur, TUNEL staining with FITC-conjugated dUTP was performed on avian H9N2-infected HBE1, and positive staining was observed in some cells at 12 hours after infection (Figure 7A). The TUNEL-positive HBE1 cells had a unique morphology compared with apoptotic cells of other lineages, and retained relatively intact nuclei (29).

We next examined the expression levels of death receptor (DR) ligands, such as the members of the TNF family. These DR ligands are responsible for the initiation of the extrinsic apoptotic pathway through TNF receptors. Among three DR ligands, the induction of TNF-α was not detected in infected TBE cells initially. FasL and TRAIL were upregulated at 6 hours after infection (3.9-fold and 5.4-fold, respectively) and 12 hours after infection (15.9-fold and 3.7-fold, respectively). At 24 hours after infection, the levels of TRAIL, FasL, and TNF-α were upregulated up to 114.6-fold, 32-fold, and 46.5-fold, respectively (Figure 7B), suggesting that DR-mediated apoptotic pathways may be activated by all three DR ligands.

To quantify the percentage of apoptotic cells in infected HBE1 cultures, we stained avian H9N2–infected cells with FITC-conjugated annexin V and PI, followed by cytometric analysis. Our data show that HBE1 cells underwent apoptosis at early stages of infection. Annexin V–positive staining was seen in 12.5% of cells at 12 hours after infection, and increased up to 18.4% at 18 hours after infection In comparison, necrotic cells comprised a larger proportion of the dead cell population during later stages of infection, with 22.6% of cells PI-positive at 18 hours after infection (data not shown).

Substrate Cleavage and Caspase Activation

To understand the mechanisms of apoptosis triggered in H9N2-infected TBE cells, we examined substrate cleavage and caspase activation, which are involved in either extrinsic (DR-mediated)

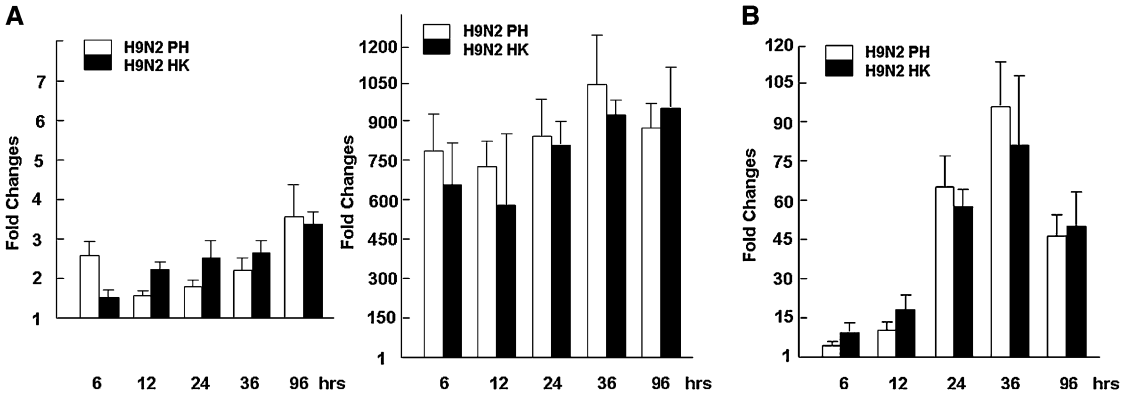

Figure 3. Induction of IFNs and IFN-inducible genes in apically differentiated TBE cultures. Real-time RT-PCR analysis was performed to examine gene-expression levels. Total RNA was prepared from virus-infected cultures at different time points after infection, and used for reverse transcription. Fold changes were calculated based on the difference in C_t values for a particular gene in uninfected and infected cells, which were normalized against glyceraldehyde-3-phospate dehydrogenase (GAPDH). Reactions were conducted in duplicate for each sample. Each reaction was repeated for at least three times, and a representative result is presented. (*A*) Fold changes in expression levels for IFN-α (*left*) and IFN-β (*right*) genes at 6, 12, 24, 36, and 96 hours after infection. (*B*) Fold changes in expression levels for myxovirus resistance 1 (Mx1) at 6, 12, 24, 36, and 96 hours after infection.

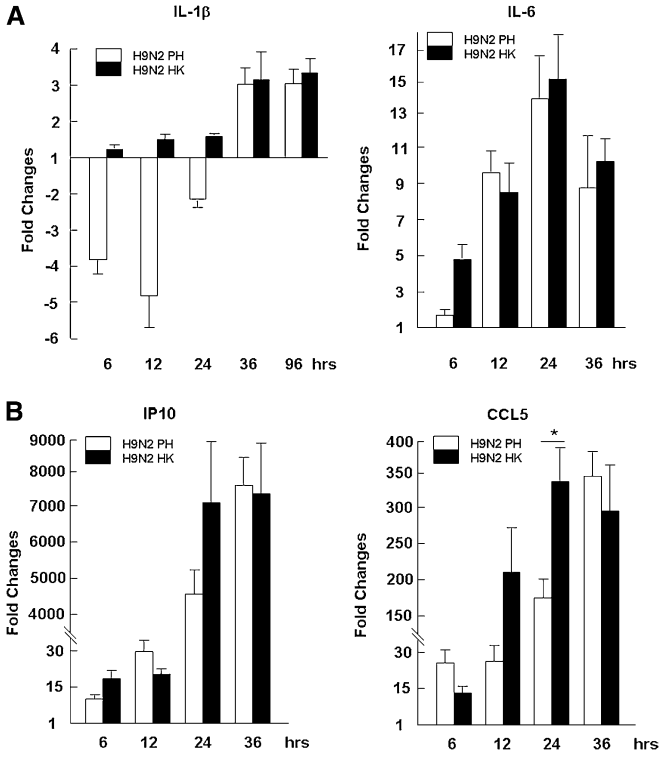

Figure 4. Differential expression of proinflammatory cytokines and chemokines in primary TBE cultures. Total RNA was prepared from virus-infected cultures at different time points after infection and used for real-time RT-PCR analysis. Reactions were conducted in duplicate, each reaction was repeated for at least three times, and a representative result is presented. (*A*) Fold changes in expression levels for IL-1β and IL-6. (*B*) Fold changes in expression levels for interferon gamma-induced protein 10 kDa (IP-10) and chemokine (C-C motif) ligand (CCL)-5 (*$P < 0.05$, *t* test; mean ± SEM).

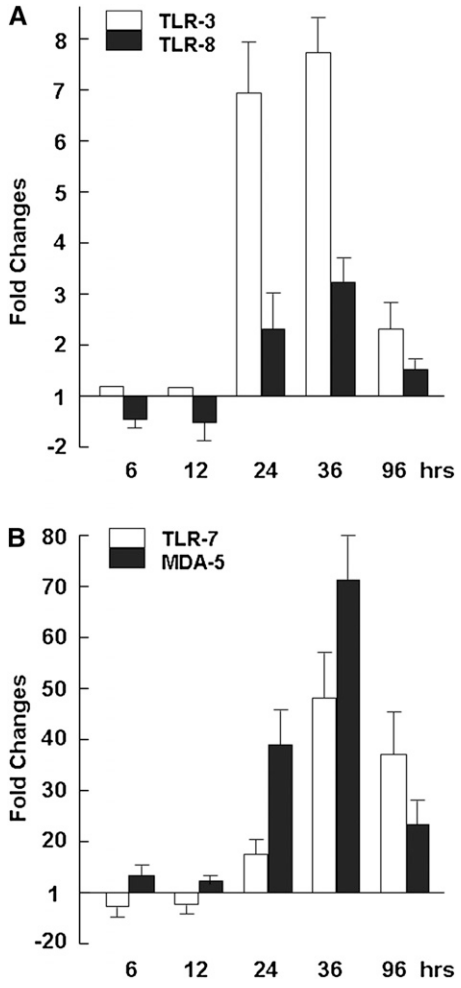

Figure 5. Regulation of TLR and MDA-5 genes in avian H9N2-infected primary TBE. Real-time RT-PCR analysis was performed to determine the changes of a few pathogen sensor receptor gene–expression levels. Reactions were performed in duplicate for each gene, and each reaction was repeated at least three times. Fold changes were calculated based on the difference in threshold of cycle [C_T] values for a particular gene in uninfected and infected cells, which were normalized against GAPDH. (*A*) Fold changes in expression levels for TLR-3 and TLR-8. (*B*) Fold changes in expression levels for TLR-7 and MDA-5.

or intrinsic (mitochondria-mediated) apoptotic pathways, or both. An 89-kilodalton (kD) cleaved fragment of PARP, a substrate of multiple executioner caspases, was detected in both cytosolic and nucleic fractions of infected cells (Figure 8A). Similarly, we detected active enzyme fragments of all three executioner caspases (caspases 3, 6, and 7) with their 16-kD, 17-kD, and 19-kD fragments, respectively (Figure 8B).

Based on the significant induction of DR ligands, we expected to see an activation of upstream initiator caspase 8 in infected cells. We detected active caspase 8 fragments of 24 kD and 2 8 kD, which are a pair of active proteases cleaved from 50-kD and 52-kD pro-caspase 8 proteins. We also detected the 39-kD active fragment of caspase 9 in infected cells (Figure 8B). The activation of caspase 9 strongly suggested that mitochondria-mediated apoptosis was involved in H9N2-induced apoptosis. This was further confirmed by the detection of cytosolic cytochrome c released from mitochondria in infected TBE cells (Figure 8C).

To examine if the mitochondria-mediated pathway was actually activated by tBid, we examined both cytosolic and membrane fractions of H9N2-infected TBE cells. Bid is a member of the Bcl-2 family containing a BH3 domain that can be cleaved by active caspase 8. We used an anti-human Bid antibody that recognizes both full-length and cleaved Bid (30). Only the 23-kD full-length Bid protein was detected in the cytosol of both noninfected and infected TBE cells. tBid (17 kD) was not detected in either cytosolic or membrane (which included mitochondria) fractions (Figure 8D, or data not shown). This indicated that mitochondria-mediated apoptosis in H9N2-infected TBE cells seems to be independent of tBid and caspase 8 activation.

Regulation of Apoptotic Pathways in H9N2-Infected TBE Cells

To understand further how apoptotic pathways are regulated in infected human airway epithelia, cell lysates from uninfected and infected TBE cells were prepared for Western blot analyses, for the potential identification of various proteins that are recognized regulators of apoptotic pathways. We found that a 55-kD apoptotic regulator, FLIP, was downregulated in the cytosol of infected cells (Figure 9A). FLIP is a homologue of caspase 8, but is devoid of protease activity. It can dimerize with caspase 8 to form heterodimers, leading to the inactivation of active caspase 8 in DR-mediated apoptotic pathways. A decrease of FLIP appeared to enhance DR-mediated apoptosis in H9N2-infected cells.

We also examined Bcl2 family members, which are key regulators of mitochondria-mediated apoptosis, in H9N2-infected TBE cells. Bak levels did not change, but both Bax

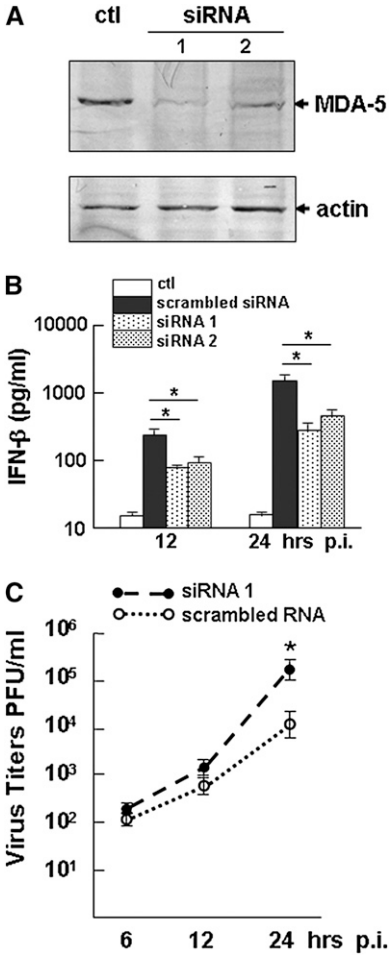

Figure 6. Knock down of melanoma differentiation–associated gene 5 (MDA-5) and IFN-β induction in HBE1 cells. (*A*) HBE1 cells were transfected with MDA-5–specific small interference (si)RNA or scrambled RNA as a control (*ctl*). Cell lysates were prepared 24 hours after transfection for Western blot analysis with an anti–MDA-5 antibody. siRNA *1* and *2* are two representative batches of cells transfected with MDA-5 siRNA. (*B*) Culture supernatants were measured by ELISA to detect secreted levels of IFN-β in avian H9N2 virus–infected HBE1 cells, which were transfected with MDA-5 siRNA and control RNA. Supernatants were taken at 12 and 24 hours after infection for ELISA (*$P < 0.05$, *t* test; mean ± SEM). (*C*) Virus titers in HBE1 cells transfected with MDA-5 siRNA and control RNA. *p.i.*, after infection. Virus titration was performed in Madin-Darby Canine Kidney (MDCK) cells by a plaque assay (*$P < 0.05$, *t* test; mean ± SEM).

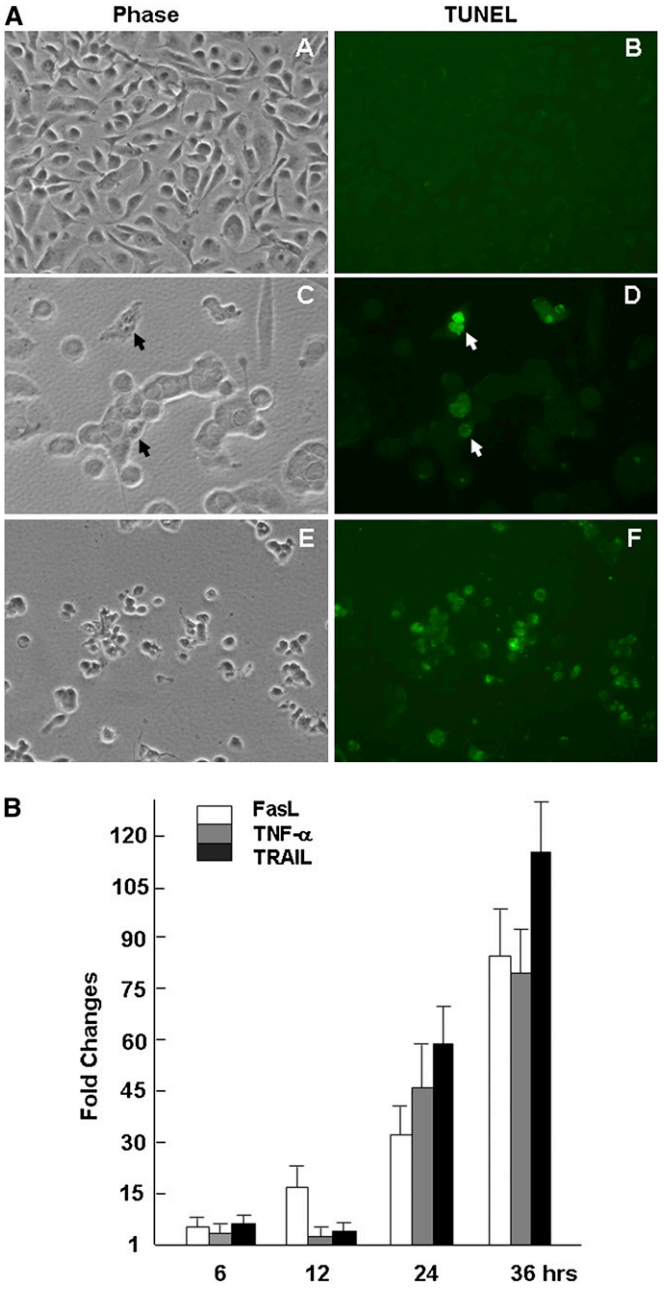

Figure 7. Apoptosis induced in avian H9N2–infected HBE1 and TBE cells. (*A*) Apoptosis of uninfected (*A* and *B*) and H9N2-infected HBE1 cultures at 12 hours (*C* and *D*) and 19 hours (*E* and *F*) after infection by an FITC-dUTP labeled Terminal deoxynucleotidyl transferase dUTP nick end labeling (TUNEL) assay. Phase contrast (*A, C,* and *E*) and fluorescence (*B, D,* and *F*) images were taken at a magnification of ×400. Apoptotic cells were indicated by arrows (*D*). (*B*) Induction of TNF family gene expressions in H9N2-infected TBE cells. Real-time RT-PCR analysis was performed to examine gene expression levels for Fas ligand (FasL), TNF-α, and TNF-related apoptosis-inducing ligand (TRAIL) at 6, 12, 24, and 36 hours after infection Reactions were conducted in duplicate for each sample, and each reaction was repeated at least three times.

and Bcl-x_s appeared to be upregulated in infected cells (Figure 9B). Some proapoptotic Bcl-2 family members, such as Bax and Bcl-x_s, are regulated by the p53 signaling pathway. To understand if p53 is activated in H9N2-infected TBE cells, we examined cell lysates with anti-phosphorylated p53 antibodies, and found that p53 was phosphorylated at serine 392 in the nuclear fraction of the infected cell lysates (Figure 9C). This finding indicates that p53 signaling is involved in the apoptotic process in H9N2-infected human TBE cells.

DISCUSSION

Avian H9N2 viruses have been widespread in domestic poultry in Asian countries since the mid-1990s, with a mortality ranging from 5–30% (31–33). Sick chickens have mild to severe respiratory signs, including edema of the head and face, and decreased egg production. Surprisingly, H9N2 strains were also identified in the human population. Initially, H9N2 was isolated from sick children in the late 1990s, and antibodies were subsequently detected in poultry workers (1, 2, 5). This indicated that the virus evolved to cross the species barrier and is

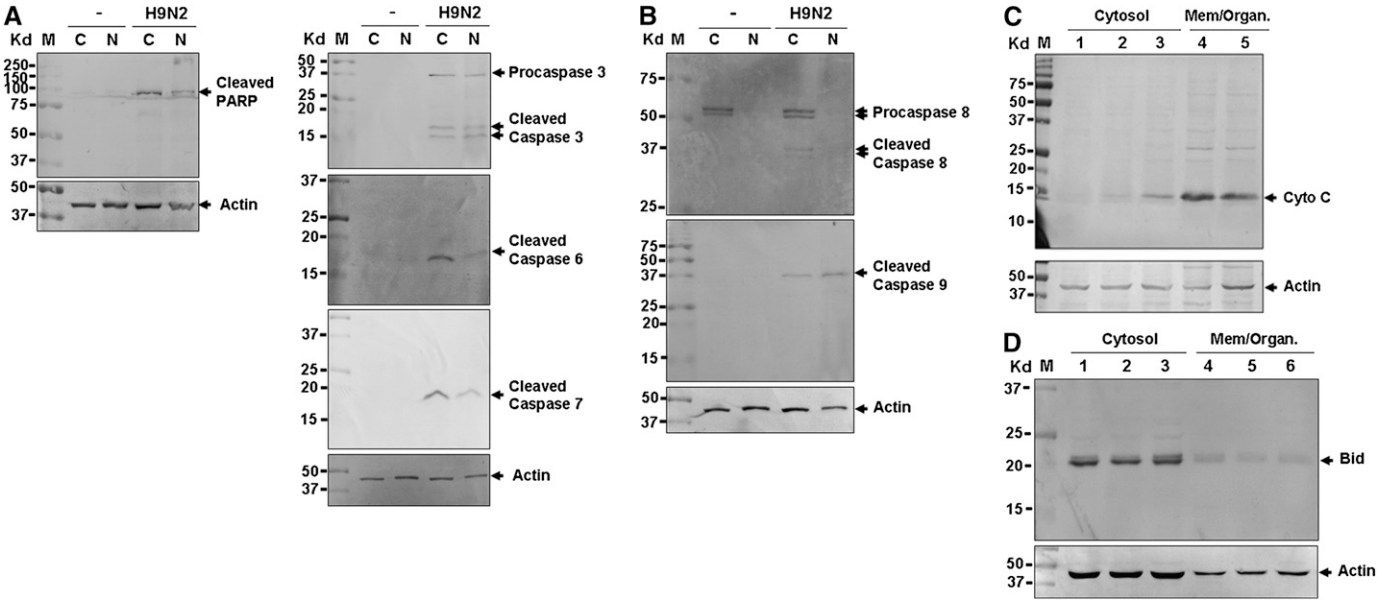

Figure 8. Both extrinsic and intrinsic apoptotic pathways were activated in avian H9N2–infected TBE cells. Cytosolic (*C*) and nuclear (*N*) fractions of cell lysates were prepared from uninfected and H9N2-infected cells at 12 hours after infection or as indicated, and fractionated in 10–15% SDS-PAGE. Subsequently, proteins were transferred to PVDF membranes for Western blot analyses. Analyses were performed at least three times for each one, and a representative result is presented. M, protein marker. (*A*) Cleavage of Poly (ADP-ribose) polymerase (PARP) and activation of executioner caspases 3, 6, and 7. (*B*) Activation of initiation caspases 8 and 9. (*C*) Release of cytochrome c into the cytosol. Cytosolic and membrane (*Mem./Organ.*) fractions of cell lysates were run in a 12% SDS-PAGE and subjected to Western blot analysis with an anti–cytochrome c antibody. (*D*) BH3 interacting domain death agonist (Bid) is not cleaved into truncated Bid (tBid) in the cytosol in infected cells. An anti-Bid antibody was used for Western blot analysis on both cytosolic and membrane fractions of cell lysates. The antibody recognizes both full-length Bid and tBid.

capable of infecting humans, bypassing intermediate hosts. Receptor-binding assays showed that the hemagglutinin (HA) of H9N2 isolates, and especially recent isolates, prefer to bind to SAα2,6Gal-linked receptors, which is also characteristic of the human H3N2 virus (16). It is important, therefore, to understand the host response patterns of H9N2 isolates in human airway epithelium, and to monitor for the emergence of newly evolved variants that possess potentially higher pathogenicity in human respiratory tissues.

Human TBE cells are primary sites for influenza virus infection, and play important roles in host defense and pathogenesis. In influenza A virus–infected respiratory epithelial cells, the induction of cytokines such as IFN-α/β, IL-6, IL-8, and chemokines (including CCL-5, chemokine (C-X-C motif) ligand (CXCL)-8, and monocyte chemotactic protein-1 (MCP-1) was observed (17, 18, 20, 21, 34). However, these studies were mainly performed in continuous or cancerous lung or bronchial cell lines grown in monolayers submerged in media favoring nondifferentiation.

We are interested in the pattern of cytokine and chemokine responses in avian H9N2–infected differentiated primary TBE cultures with an apical surface that better approximates the *in vivo* situation. A human H9N2 virus isolated from a patient in Hong Kong was used in this study for comparison, which demonstrated that the avian H9N2 virus has evolved to a stage where it can infect human bronchial epithelial cells as efficiently as a human virus. Specifically, our results showed that IFN-β was the predominant antiviral cytokine, induced up to 1,000-fold, along with the induction of IFN-inducible Mx1 and 2′5′-OAS. However, IFN-α and IFN-γ remained unchanged. Remarkably, IP-10 and CCL-5 were substantially induced upon infection, which presumably comprise the main driving force for proinflammatory responses. IP-10 and CCL-5 are key chemokines for the recruitment of blood mononuclear cells and T lymphocytes to the respiratory tract. In the presence of IL-2 and IFN-γ released from activated T cells recruited locally, CCL-5 can also induce the proliferation and activation of natural killer cells (35). Although TNF-α and IL-6 may also participate in pathogenicity, IL-1β and IL-8 were downregulated early in infection, and may constitute only minor factors.

In human primary TBE, both membrane-bound TLR and cytosolic RIG-1–like receptors were involved in the innate immune response to stimulate the production of cytokines such as antiviral IFN-β. Among TLRs, TLR-7 and TLR-3 seemed to be the main receptors induced, whereas the concentration of TLR-8 remained unchanged. The induction of TLRs was a late event, and did not commence until 24 hours after infection, but MDA-5 was induced much earlier. Using siRNA to knock down MDA-5, we demonstrated that MDA-5 is important in the induction of IFN-β, and is instrumental in the innate immunity against the H9N2 virus in human bronchial epithelial cells.

Virus-induced apoptosis can be triggered through DR-mediated extrinsic pathways, mitochondria-mediated intrinsic pathways, or both. Fas-associated protein with death domain (FADD)/caspase 8 and mitochondria/cytochrome c are crucial components of the extrinsic and intrinsic pathways, respectively. Crosstalk between the two pathways can occur through the caspase 8–mediated cleavage of Bid into tBid. tBid is subsequently translocated from the cytosol into the mitochondria, to promote the release of cytochrome c into the cytosol, which then activates caspase 9. Unlike macrophages infected with influenza A virus (29), human bronchial epithelial cells did not exhibit morphologically typical apoptosis under TUNEL staining, as shown in this study. Despite the morphologic uniqueness, molecular evidence of apoptosis did occur in infected cells, as demonstrated by the activation of all three executioner caspases (caspase 3, caspase 6, and caspase 7) and the cleavage of PARP (Figure 8). We confirm that the extrinsic apoptotic cascade was

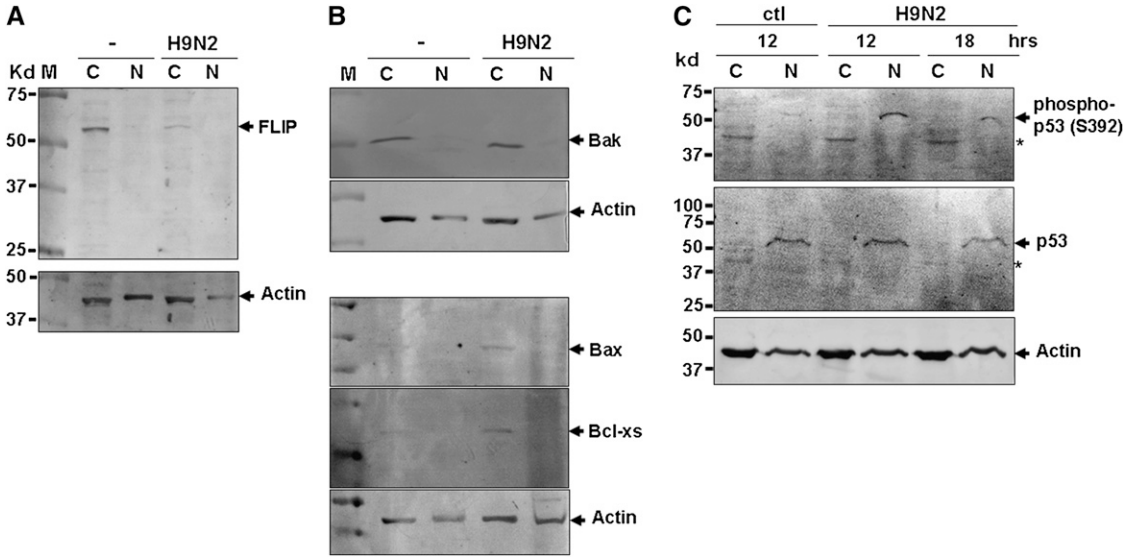

Figure 9. Involvement of FLIP and p53 signaling pathways in the regulation of apoptosis in avian H9N2–infected HBE1 and TBE cells. Cytosolic (*C*) and nuclear (*N*) fractions of cell lysates were prepared from uninfected and infected cells at 12 hours (*A* and *B*) after infection or as indicated, and fractionated on 12–15% SDS-PAGE. Proteins were transferred to PDVF membranes before they were blotted with specific antibodies. Each analysis was performed at least three times, and a representative result is presented. (*A*) FLIP was downregulated in infected cells. (*B*) Bcl-2 family members Bax and Bcl-x_s were upregulated in infected cells. (*C*) p53 was phosphorylated at serine 392 in H9N2-infected cells. *Arrows* indicate phosphorylated p53 bands. *Nonspecific bands, shown in both infected and noninfected cells by the antibody.

clearly activated in human bronchial epithelial cells infected with H9N2 virus, as demonstrated by the presence of cleaved and active caspase 8. Active caspase 8 will cleave and activate downstream caspase 3, leading to subsequent substrate cleavages. Importantly, our data unambiguously reveal that cytosolic cytochrome c levels were increased, and that zymogen procaspase 9 was cleaved and activated in infected cells, indicating that the intrinsic apoptotic cascade was also activated. We determined that the activation of caspase 9–mediated apoptosis does not occur through the caspase 8–mediated cleavage of Bid. The intrinsic pathway is very likely triggered by proapoptotic Bcl-2 family members, because we detected the upregulation of p53-dependent Bax and Bcl-x_s in the cytosol, and moreover, p53 was phosphorylated at serine 392 in the nuclei of infected cells. This finding suggests that the mitochondria/cytochrome–mediated apoptosis in H9N2-infected human airway epithelial cells may occur via the p53-dependent signaling pathway, activated in the nucleus where influenza virus replicates.

Little was previously known about the involvement of the mitochondria/cytochrome c–mediated apoptotic pathway in influenza-infected human bronchial epithelial cells. Previous studies showed that the overexpression of NS1 protein in NCI-H292 cells, a human cell line derived from mucoepidermoid lung carcinoma, led to apoptosis, but had no effect on Bid, Bim, Bad, Bcl-x_L, or caspase 9 (26). Influenza virus encodes a PB1-F2 protein, which seems to target the mitochondria specifically and cause apoptosis (36–39). However, PB1-F2 is unlikely to be the cause of the mitochondria/cytochrome c–mediated apoptosis induced in H9N2-infected HBE culture. First, the overexpression of PB1-F2 by transfection can cause apoptosis, mainly in monocytic cells, but none or little in epithelial cells (36, 37). Moreover, no studies have shown whether this cell type–restricted apoptosis can be induced by the PB1-F2 produced in virally infected cells. Second, the expression of PB1-F2 by transfection seems able to enhance TNF-α–induced apoptosis in epithelial A549 and 293T cell lines (36). In our study, however, TNF-α was significantly induced only at a late stage of infection (24 hours after infection (Figure 7B), long after the release of cytochrome c into the cytosol (earlier than 16 hours after infection). Third, PB1-F2–induced apoptotic sensitization appears to be associated with an augmentation of tBid-induced cytochrome c release (36), whereas no tBid was detected in H9N2-infected human HBE cells in this study.

Both extrinsic and intrinsic apoptotic cascades are tightly regulated. The regulators include Bcl-2 family members, inhibitor of apoptosis proteins, and others (e.g., FLIP). p53 can be activated through phosphorylation at serine 392, which is also the cellular response to ultraviolet irradiation (40–42), leading to either apoptosis or growth arrest. We observed an increase of p53 serine 392 phosphorylation in influenza-infected human HBE cells, and this increase may have regulated the Bcl-2 family members and triggered mitochrondria/cytochrome c–mediated apoptosis. FLIP is a structural homologue of procaspase 8 and a dual regulator of the extrinsic apoptotic pathway. It does not exert proteolytic activity because of its inactive enzymatic structure. However, FLIP can bind with procaspase 8 to form heterodimers. When FLIP is overexpressed, heterodimerization can result in the blockage of pro-caspase 8 activation. But as shown previously under physiologic conditions, FLIP–pro-caspase 8 heterodimerization may enhance the cleavage and activation of pro-caspase 8 (43). Therefore, the downregulation of FLIP in H9N2-infected human TBE would lead to decreased apoptosis, which is a potential strategy used by influenza viruses to suppress apoptosis in infected cells. Attempts are underway to uncover the mechanisms of how FLIP is downregulated in human HBEs.

Author Disclosure: R.H. received a sponsored grant (HL085311) from the National Institutes of Health for more than $100,001. None of the other authors has a financial relationship with a commercial entity that has an interest in the subject of this manuscript.

Acknowledgments: This study was supported by grants from the Department of Homeland Security National Center for Foreign Animal and Zoonotic Disease Defense (C.J.C. and Z.X). Z.X. was also supported by the National Natural Science Foundation of China (grant 30971450/C0703) and the State Key Laboratory of Pharmaceutical Biotechnology of Nanjing University (grant KF-GW-200902).

References

1. Peiris M, Yuen KY, Leung CW, Chan KH, Ip PL, Lai RW, Orr WK, Shortridge KF. Human infection with influenza H9N2. *Lancet* 1999; 354:916–917.

2. Butt KM, Smith GJ, Chen H, Zhang LJ, Leung YH, Xu KM, Lim W, Webster RG, Yuen KY, Peiris JS, *et al.* Human infection with an avian H9N2 influenza a virus in Hong Kong in 2003. *J Clin Microbiol* 2005;43:5760–5767.
3. Lin YP, Shaw M, Gregory V, Cameron K, Lim W, Klimov A, Subbarao K, Guan Y, Krauss S, Shortridge K, *et al.* Avian-to-human transmission of H9N2 subtype influenza a viruses: relationship between H9N2 and H5N1 human isolates. *Proc Natl Acad Sci USA* 2000;97:9654–9658.
4. Guan Y, Shortridge KF, Krauss S, Chin PS, Dyrting KC, Ellis TM, Webster RG, Peiris M. H9N2 influenza viruses possessing H5N1-like internal genomes continue to circulate in poultry in southeastern China. *J Virol* 2000;74:9372–9380.
5. Guo Y, Li J, Cheng X. Discovery of men infected by avian influenza A (H9N2) virus *Zhonghua Shi Yan He Lin Chuang Bing Du Xue Za Zhi* 1999;13:105–108 (in Chinese).
6. Shortridge KF, Gao P, Guan Y, Ito T, Kawaoka Y, Markwell D, Takada A, Webster RG. Interspecies transmission of influenza viruses: H5N1 virus and a Hong Kong SAR perspective. *Vet Microbiol* 2000;74:141–147.
7. Subbarao K, Katz J. Avian influenza viruses infecting humans. *Cell Mol Life Sci* 2000;57:1770–1784.
8. Liu J, Okazaki K, Ozaki H, Sakoda Y, Wu Q, Chen F, Kida H. H9N2 influenza viruses prevalent in poultry in china are phylogenetically distinct from A/quail/Hong Kong/G1/97 presumed to be the donor of the internal protein genes of the H5N1 Hong Kong/97 virus. *Avian Pathol* 2003;32:551–560.
9. Brydon EW, Smith H, Sweet C. Influenza A virus-induced apoptosis in bronchiolar epithelial (NCI-H292) cells limits pro-inflammatory cytokine release. *J Gen Virol* 2003;84:2389–2400.
10. Chan MC, Cheung CY, Chui WH, Tsao SW, Nicholls JM, Chan YO, Chan RW, Long HT, Poon LL, Guan Y, *et al.* Proinflammatory cytokine responses induced by influenza A (H5N1) viruses in primary human alveolar and bronchial epithelial cells. *Respir Res* 2005;6:135.
11. Ibricevic A, Pekosz A, Walter MJ, Newby C, Battaile JT, Brown EG, Holtzman MJ, Brody SL. Influenza virus receptor specificity and cell tropism in mouse and human airway epithelial cells. *J Virol* 2006;80:7469–7480.
12. Kogure T, Suzuki T, Takahashi T, Miyamoto D, Hidari KI, Guo CT, Ito T, Kawaoka Y, Suzuki Y. Human trachea primary epithelial cells express both sialyl(alpha2–3)Gal receptor for human parainfluenza virus type 1 and avian influenza viruses, and sialyl(alpha2–6)Gal receptor for human influenza viruses. *Glycoconj J* 2006;23:101–106.
13. Matrosovich MN, Matrosovich TY, Gray T, Roberts NA, Klenk HD. Human and avian influenza viruses target different cell types in cultures of human airway epithelium. *Proc Natl Acad Sci USA* 2004;101:4620–4624.
14. Matrosovich MN, Matrosovich TY, Gray T, Roberts NA, Klenk HD. Neuraminidase is important for the initiation of influenza virus infection in human airway epithelium. *J Virol* 2004;78:12665–12667.
15. Thompson CI, Barclay WS, Zambon MC, Pickles RJ. Infection of human airway epithelium by human and avian strains of influenza A virus. *J Virol* 2006;80:8060–8068.
16. Wan H, Perez DR. Amino acid 226 in the hemagglutinin of H9N2 influenza viruses determines cell tropism and replication in human airway epithelial cells. *J Virol* 2007;81:5181–5191.
17. Choi AM, Jacoby DB. Influenza virus A infection induces interleukin-8 gene expression in human airway epithelial cells. *FEBS Lett* 1992;309:327–329.
18. Adachi M, Matsukura S, Tokunaga H, Kokubu F. Expression of cytokines on human bronchial epithelial cells induced by influenza virus A. *Int Arch Allergy Immunol* 1997;113:307–311.
19. Matsukura S, Kokubu F, Kubo H, Tomita T, Tokunaga H, Kadokura M, Yamamoto T, Kuroiwa Y, Ohno T, Suzaki H, *et al.* Expression of RANTES by normal airway epithelial cells after influenza virus A infection. *Am J Respir Cell Mol Biol* 1998;18:255–264.
20. Matsukura S, Kokubu F, Noda H, Tokunaga H, Adachi M. Expression of IL-6, IL-8, and RANTES on human bronchial epithelial cells, NCI-H292, induced by influenza virus A. *J Allergy Clin Immunol* 1996;98:1080–1087.
21. Ronni T, Matikainen S, Sareneva T, Melen K, Pirhonen J, Keskinen P, Julkunen I. Regulation of IFN-alpha/beta, MXA, 2′,5′-oligoadenylate synthetase, and HLA gene expression in influenza A–infected human lung epithelial cells. *J Immunol* 1997;158:2363–2374.
22. Bateman AC, Busch MG, Karasin AI, Bovin N, Olsen CW. Amino acid 226 in the hemagglutinin of H4N6 influenza virus determines binding affinity for alpha2,6–linked sialic acid and infectivity levels in primary swine and human respiratory epithelial cells. *J Virol* 2008;82:8204–8209.
23. Takizawa T, Matsukawa S, Higuchi Y, Nakamura S, Nakanishi Y, Fukuda R. Induction of programmed cell death (apoptosis) by influenza virus infection in tissue culture cells. *J Gen Virol* 1993;74:2347–2355.
24. Takizawa T, Fukuda R, Miyawaki T, Ohashi K, Nakanishi Y. Activation of the apoptotic FAS antigen-encoding gene upon influenza virus infection involving spontaneously produced beta-interferon. *Virology* 1995;209:288–296.
25. Balachandran S, Roberts PC, Kipperman T, Bhalla KN, Compans RW, Archer DR, Barber GN. Alpha/beta interferons potentiate virus-induced apoptosis through activation of the FADD/caspase-8 death signaling pathway. *J Virol* 2000;74:1513–1523.
26. Lam W Y, Tang JW, Yeung AC, Chiu LC, Sung JJ, Chan PK. Avian influenza virus A/HK/483/97(H5N1) NS1 protein induces apoptosis in human airway epithelial cells. *J Virol* 2008;82:2741–2751.
27. Woolcock PR, Suarez DL, Kuney D. Low-pathogenicity avian influenza virus (H6N2) in chickens in California, 2000–02. *Avian Dis* 2003;47(Suppl 3):872–881.
28. Yankaskas JR, Haizlip JE, Conrad M, Koval D, Lazarowski E, Paradiso AM, Rinehart CA Jr, Sarkadi B, Schlegel R, Boucher RC. Papilloma virus immortalized tracheal epithelial cells retain a well-differentiated phenotype. *Am J Physiol* 1993;264:C1219–C1230.
29. Xing Z, Cardona CJ, Li J, Dao N, Tran T, Andrada J. Modulation of the immune responses in chickens by low-pathogenicity avian influenza virus H9N2. *J Gen Virol* 2008;89:1288–1299.
30. Baumann R, Casaulta C, Simon D, Conus S, Yousefi S, Simon HU. Macrophage migration inhibitory factor delays apoptosis in neutrophils by inhibiting the mitochondria-dependent death pathway. *FASEB J* 2003;17:2221–2230.
31. Guan Y, Shortridge KF, Krauss S, Webster RG. Molecular characterization of H9N2 influenza viruses: were they the donors of the "internal" genes of H5N1 viruses in Hong Kong? *Proc Natl Acad Sci USA* 1999;96:9363–9367.
32. Chen BL, Zhang ZJ, Chen W. Isolation and identification of avian influenza virus. *Chin J Vet Med* 1994;10:3–5.
33. Cameron KR, Gregory V, Banks J, Brown IH, Alexander DJ, Hay AJ, Lin YP. H9N2 subtype influenza A viruses in poultry in Pakistan are closely related to the H9N2 viruses responsible for human infection in Hong Kong. *Virology* 2000;278:36–41.
34. Julkunen I, Melen K, Nyqvist M, Pirhonen J, Sareneva T, Matikainen S. Inflammatory responses in influenza A virus infection. *Vaccine* 2000;19:S32–S37.
35. Maghazachi AA, Al-Aoukaty A, Schall TJ. CC chemokines induce the generation of killer cells from $CD56^+$ cells. *Eur J Immunol* 1996;26:315–319.
36. Zamarin D, Garcia-Sastre A, Xiao X, Wang R, Palese P. Influenza virus PB1-F2 protein induces cell death through mitochondrial ANT3 and VDAC1. *PLoS Pathog* 2005;1:e4.
37. Chen W, Calvo PA, Malide D, Gibbs J, Schubert U, Bacik I, Basta S, O'Neill R, Schickli J, Palese P, *et al.* A novel influenza A virus mitochondrial protein that induces cell death. *Nat Med* 2001;7:1306–1312.
38. Gibbs JS, Malide D, Hornung F, Bennink JR, Yewdell JW. The influenza A virus PB1-F2 protein targets the inner mitochondrial membrane via a predicted basic amphipathic helix that disrupts mitochondrial function. *J Virol* 2003;77:7214–7224.
39. Yamada H, Chounan R, Higashi Y, Kurihara N, Kido H. Mitochondrial targeting sequence of the influenza A virus PB1-F2 protein and its function in mitochondria. *FEBS Lett* 2004;578:331–336.
40. Kapoor M, Lozano G. Functional activation of p53 via phosphorylation following DNA damage by UV but not gamma radiation. *Proc Natl Acad Sci USA* 1998;95:2834–2837.
41. Lu H, Taya Y, Ikeda M, Levine AJ. Ultraviolet radiation, but not gamma radiation or etoposide-induced DNA damage, results in the phosphorylation of the murine p53 protein at serine-389. *Proc Natl Acad Sci USA* 1998;95:6399–6402.
42. Keller DM, Zeng X, Wang Y, Zhang QH, Kapoor M, Shu H, Goodman R, Lozano G, Zhao Y, Lu HA. DNA damage-induced p53 serine 392 kinase complex contains CK2, HSPT16, and SSRP1. *Mol Cell* 2001;7:283–292.
43. Chang DW, Xing Z, Pan Y, Algeciras-Schimnich A, Barnhart BC, Yaish-Ohad S, Peter ME, Yang X. C-FLIP(l) is a dual function regulator for caspase-8 activation and CD95-mediated apoptosis. *EMBO J* 2002;21:3704–3714.